UNIVERSIDADE DE LISBOA
FACULDADE DE CIÊNCIAS
DEPARTAMENTO DE MATEMÁTICA

**Ciências
ULisboa**

Analysis of the Rosenzweig-MacArthur Model with Bifurcation Structures and Stochastic Processes

Pablo Elías Fuentes Sommer

Mestrado em Matemática

Disertação orientada por:
Prof. Nico STOLLENWERK

2016

Abstract

The Rosenzweig-MacArthur is one of the simplest models in populational biology to present a Hopf bifurction. By adding seasonal variation to the model the fixed point on one side of the Hopf bifurcation becomes a limit cycle and, on the other side of the bifurcation, the Hopf limit cycle is transformed into a torus, therefore the Hopf bifurcation becomes a torus bifurcation, and soon deterministic chaos can follow via torus destruction. We examine this route to chaos including stochastic versions that would be the only processes observed in real world systems.

This study shows the torus destruction into chaos with positive Lyapunov exponents. This chaotic behaviour is observed in parameter regions where also a time scale separation is possible, which enables stochastic versions of the model. The chaotic dynamics are observed inside Arnol'd tongues on the torus.

Homologous bifurcation structures and torus destruction into chaos arise also in other population biological systems. These models, specially when studying real world data, are usually highly complex. Accordingly, the presented analysis can be used as a study case for more complex systems also in view of the stochastic modeling.

Keywords: Rosenzweig-MacArthur model, torus bifurcation, stochastic systems, stoichiometric formulation, deterministic chaos, Lyapunov spectrum

Dedication

This thesis is dedicated to all the people who in any form have supported and accompanied me throughout my life.

Specially, I would like to dedicate this work to my mother Irmtraud, my father David, my two sisters Thea and Emilia and the whole Fuentes family who have been an unconditional source of love, kindness and support.

Also, an extraordinary thanks to Brigitte, Manuel, Leopold, Max and Paul. They have become an exceptional part of my life ever since I first arrived to their family.

And an utmost significant thanks goes to Mieke for being always loving and supportive, being so far away and yet so close.

Acknowledgements

I would like to express my most profound appreciation to Prof. Nico Stollenwerk for his guidance through my Master's degree studies and specially while supervising this thesis. Without his counseling and mentoring through all the stages of this work, this thesis would not have been possible.

I am also grateful to the Biomathematics and Statistics Group of CMAF-CIO. Luís Mateus, Maíra Aguiar, Peyman Ghaffari and Raquel Filipe who have conributed to this work with valuable knowledge and interesting discussions about etymology whenever appropiate.

Fundação da Ciência e Tecnología made the research of this work possible through a scientific research fellowship.

Contents

Resumo

Muitos modelos matemáticos utilizados na investigação científica da biologia populacional e da epidemiologia exibem comportamento determinístico dinâmico caótico emergindo de bifurcações no toro e além disso da destruição do atrator do toro. Estes modelos são geralmente bastante complexos e possuem dimensão elevada, consequentemente, o estudo de tais dinâmicas não é bastante intuitivo nestes modelos. Então um modelo mais simples, de dimensão menor, que exibe essas propriedades deve ser analisado para obter a análise mais pormenorizada do comportamento caótico de modelos complexos.

Na dinâmica populacional, uma bifurcação no toro geralmente ocorre quando se considera a variação sazonal de um dos parâmetros de um sistema que já exibe uma bifurcação de Hopf na sua dinâmica.

O principal objetivo da presente dissertação é estudar o comportamento dinâmico de um modelo predador-presa que apresenta uma bifurcação de Hopf. E, adicionando ainda mais complexidade ao modelo, pretende-se continuar uma análise das crescentes bifurcações no toro e do caos determinístico próximos da destruição do toro.

Um dos modelos populacionais biológicos mais simples exibindo uma bifurcação de Hopf é o modelo Rosenzweig-MacArthur, devido à sua não linearidade cúbica proveniente da função de resposta Holling tipo II por meio de uma transformação orbitalmente equivalente. Assim, começamos por introduzir as equações de Lotka-Volterra para descrever modelos predador-presa e a categorização de funções de resposta por Holling em tipo I, II e III.

No entanto, a função de resposta Holling tipo II, que neste modelo permite uma bifurcação de Hopf, devido à não linearidade cúbica observada, não está diretamente relacionada com a transição de uma classe de população para outra que permita uma versão estocástica automaticamente. Em vez disso, um argumento de separação de escala de tempo conduz ao modelo simples bidimensional Rosenzweig-MacArthur a partir de um modelo mais complexo, através de classes adicionais de predadores em digestão de alimen-

tos e predadores em busca de presas. Isto significa que os predadores mudam o seu estado de busca para manuseio quando capturam uma presa dependendo da população das presas e da própria taxa de caça dos predadores. Os predadores que capturaram uma presa irão levar algum tempo para lidar com ela e digeri-la, enquanto neste estado de manuseio um predador não procura nem captura qualquer presa. Além disso, assume-se que as presas consomem algum tipo de recurso ou espaço, a fim de procriar. Este recurso ou o espaço é limitado, portanto, a soma da população de presas e de recursos/espaço disponível é constante.

Este modelo estendido permite uma generalização estocástica com a versão estocástica de uma bifurcação de Hopf, e, finalmente, também com a sazonalidade adicional que permite uma bifurcação no toro. Calcularam-se os estados estacionários do modelo reduzido bidimensional e do modelo tridimensional estendido. Também foi feita uma análise de estabilidade de ambos os sistemas que foi realizada através de matrizes Jacobianas e avaliação valores próprios. As simulações deterministas foram então conduzidas com um determinado conjunto de parâmetros que onde se encaixa o argumento de separação de escala.

A simulação estocástica foi realizada em primeiro lugar na forma de uma equação de perda-ganho para as probabilidades de estados separados, a equação mestre. No entanto, a aproximação da equação mestre provou ser computacionalmente exigente e uma vez que para uma análise mais aprofundada dos expoentes de Lyapunov, esta simulação precisa ser calculada repetitivamente, portanto, seria necessária uma simulação mais rápida. Por isso, introduziu-se um tipo especial de equação mestre, a equação diferencial Fokker-Planck. Esta é derivada como uma expansão de Taylor na equação mestre com densidades. Isto permitiu simulações mais rápidas que são apropriadas para os próximos cálculos pesados dos expoentes de Lyapunov.

Introduziu-se uma variação sazonal no modelo, ambos com forçamento sazonal direto e por extensão em um sistema de quatro dimensões através do oscilador de Hopf. O oscilador de Hopf prova ser uma ferramenta mais adequada para simular sazonalidade do que uma aproximação mais usual com um oscilador harmônico, devido ao oscilador de Hopf convergir para um ciclo limite de quaisquer de condições iniciais. Isto não seria viável com um oscilador harmônico, onde as variações estocásticas e também erros numéricos levam a saltos em diferentes trajetórias com diferentes ciclos limites como soluções.

O parâmetro escolhido aqui para flutuar periodicamente com um oscilador de Hopf foi a taxa de caça do predador. O que implica que, num modelo de biologia populacional, os predadores caçam presas mais depressa e mais facilmente durante certas épocas do ano. Isso também coincide com estudos

anteriores realizados na dinâmica caótica das modelos predador-presa.

Em versões sazonalmente forçadas o ponto fixo da bifurcação de Hopf, por um lado torna-se um ciclo limite, e por outro o ciclo limite de Hopf torna-se um toro, por conseguinte, a bifurcação de Hopf torna-se uma bifurcação no toro, e através da destruição do toro o parâmetro espaço pode seguir caos determinístico. Investigou-se essa rota para o caos também no ponto de vista de versões estocásticas, já que em sistemas do mundo real seriam observados apenas esses processos estocásticos.

Além disso realizou-se uma análise do espectro de Lyapunov como um conjunto de expoentes. O espectro de Lyapunov é uma boa caracterização da taxa de separação de trajetórias com partida nas condições iniciais vizinhas.

O espectro de Lyapunov fornece informações relevantes sobre o comportamento dinâmico do sistema. Assim, quando todos os expoentes de Lyapunov são negativos, as trajetórias a partir de condições iniciais vizinhas estão-se a aproximar com o tempo, e, por exemplo, aparecerem pontos fixos. Se o maior expoente de Lyapunov for igual a zero, então, as trajetórias são estão-se a aproximar numa única direção e a separação é constante na outra direção, portanto, podem aparecer ciclos limite e uma bifurcação está a ocorrer pelo meio. E se pelo menos um dos expoentes é positivo, então, pelo menos, numa direçã as trajetórias das condições iniciais vizinhas estão a crescer, por conseguinte, a dinâmica do sistema será caótica.

Os expoentes Lyapunov podem ser calculados através de uma decomposição do produto de matrizes Jacobianas ao longo de uma órbita. Este produto de matrizes é decomposto numa matriz ortonormal e numa matriz triangular superior direita. Onde a matriz ortonormal transporta a informação sobre a direção da divergência entre as trajetórias, enquanto a matriz triangular superior direito transporta, principalmente nos seus elementos diagonais, a taxa de separação real em cada direção da matriz ortonormal. Durante a realização de um cálculo numérico do espectro de Lyapunov em algumas regiões de parâmetros surgem saltos inesperados na curva de outro modo relativamente suave do espectro. Estes saltos aparecem especificamente em simulações com a variação sazonal de uma força relativamente pequena. As irregularidades tornam-se saltos sobre as trajetórias entre atratores coexistentes. Para evitar estes saltos entre atratores os valores inicíais das simulações são modificados, para que seja possível ficar próximo de um atrator sem saltar para trajetórias vizinhas que estão na bacia de atração de um atrator diferente.

O presente estudo mostra que a destruição do toro no caos com expoentes de Lyapunov positivos pode ocorrer em regiões de parâmetros onde também é possível a separação da escala de tempo e, portanto versões estocásticos

3

do modelo. O movimento caótico é observado dentro línguas de Arnol'd de valores racionais da frequência de forçamento e da frequência própria do ciclo limite de Hopf não forçado. Tais bifurcações no toro e destruição do toro em caos também são observados noutros sistemas biológicos populacionais, e foram, por exemplo, encontrados em modelos epidemiológicos estendidos de varias estirpes sobre a dengue. Para entender tais cenários dinâmicos melhor também sob perturbações, o atual sistema de baixa dimensão pode servir como um bom caso de estudo.

Palavras-chave: modelo de Rosenzweig-MacArthur, bifurcação de torus, sistemas estocásticos, formulação estoquiométrica, caos determinístico, espectro de Lyapunov

Introduction

Many mathematical models used in the scientific research of population biology and epidemiology display deterministic chaotic dynamical behavior emerging from torus bifurcations and further destruction of the torus attractor itself. These models are usually rather complex and high dimensional, consequently the study of such dynamics is not quite intuitive in these models. Thereupon a lower dimensional simpler model that displays these properties should be analyzed to get a more detailed insight into the chaotic behavior of complex models.

In population dynamics, a torus bifurcation usually occurs when considering seasonal variation of one of the parameters of a system that already displays a Hopf bifurcation in its dynamics.

The main objective of the present thesis is to study the dynamical behavior of a predator-prey model which displays a Hopf bifurcation. And by adding further complexity to the model we aim to perform an analysis of uprising torus bifurcations and deterministic chaos upcoming from torus destruction.

In chapter one we start by introducing the Lotka-Volterra equations to describe predator-prey models. We perform a short analysis on the stationary states and the categorization of response functions by Holling into type I, II and III.

Further we present the model to be analyzed. It is a predator-prey model in which the predators are divided in two exclusive states of food handling and prey searching. This means the predators change their state from searching into handling when they successfully catch a prey depending on the prey population and the own hunting rate of the predators. Predators that have caught a prey will take some time to handle and digest it, while in this handling state a predator does not search nor catch any prey. Additionally, the prey are assumed to consume some kind of resource or space in order to procreate. This resource or space is limited, thus the sum of prey population and resource/space available is constant.

However, the Holling type II response function, which in this model allows a Hopf bifurcation due to the upcoming cubic nonlinearity, is not directly related to a transition from one to another population class which would allow a stochastic version straight away. Instead, a time scale separation argument leads from a more complex model to the simple two dimensional Rosenzweig-MacArthur model.

We compute the stationary states of both, the reduced two dimensional model and the extended three dimensional model. Also a stability analysis of both systems is conducted via Jacobian matrices and eigenvalues evaluation. Deterministic simulations are then conducted with a given parameter set that fits the scale separation argument.

The extended model presented in chapter one allows a stochastic generalization with the stochastic version of a Hopf bifurcation, and ultimately also with additional seasonality allowing a torus bifurcation. Thus, chapter two focusses in the stochastic simulations of the model.

First, the stochastic simulation is realized as a gain-loss equation for the probabilities of the separate states, the master equation. Nevertheless, the master equation approach proves to be computationally expensive and since for further analysis of the Lyapunov exponents, this simulation needs to be computed repetitively, a faster simulation is required. Hence we introduce a special type of master equation, the Fokker-Planck differential equation. It is derived as a Taylor's expansion on the Master equation with densities. This will allow us faster simulations which will be appropriate for the upcoming heavy calculations of the Lyapunov exponents.

The results of chapters one and two have been presented by the author at the Seventh Workshop in Dynamichal Systems Applied to Biological Sciences in Évora in 2016. The results were also published in conference contributions at the International Conference in Numerical Analysis and Applied Mathematics in Rhodes, Greece in 2015[15] and at the Proceedings of the 15th International Conference on Mathematical Methods in Science and Engeneering in Cádiz, Spain in 2015 [6].

In chapter three we introduce seasonal variation in the model, both with direct seasonal forcing and by extension into a four dimensional system via Hopf oscillator. The Hopf oscillator proves to be a more adequate tool to simulate seasonality than a more usual approach with an harmonic oscillator due to the Hopf oscillator converging into one limit cycle from any set of initial conditions.This would not be feasible with an harmonic oscillator where the stochastic variations and also numerical errors lead to jumps into different trajectories with different limit cycles as solutions.

The parameter chosen here to fluctuate periodically with a Hopf oscillator is the predator hunting rate. Which implies that, in a population biology model, predators hunt prey faster and easier during certain seasons of the year. This also matches previous studies performed on chaotic dynamics of predator-prey models.

In seasonally forced versions the fixed point on one side of the Hopf bifurcation becomes a limit cycle and the Hopf limit cycle on the other hand becomes a torus, hence the Hopf bifurcation becomes a torus bifurcation, and via torus destruction soon deterministic chaos can follow in parameter space. We investigate this route to chaos also in view of stochastic versions, since in real world systems only such stochastic processes would be observed.

Additionally, in chapter four, we carry out an analysis of the Lyapunov spectrum as a set of exponents. The Lyapunov spectrum is a good characterization of the rate of separation of trajectories starting at neighboring initial conditions.

The Lyapunov spectrum delivers relevant information about the dynamical behavior of the system. Hence, when all Lyapunov exponents are negative, the trajectories starting from neighboring initial conditions are getting closer with the time, e.g. fix points appear. If the biggest Lyapunov exponent is equal to zero, then the trajectories are getting closer only in one direction and the separation is being constant in the other direction, hence limit cycles appear and a bifurcation is happening in between. And if at least one of the exponents is positive, then at least in one direction the trajectories of neighboring initial conditions are growing apart, hence the dynamics of the system are chaotic.

The Lyapunov exponents can be computed through a decomposition of the product of Jacobian matrices along an orbit. This product matrix is decomposed into an orthonormal matrix and an upper right triangular matrix. In this decomposition, the orthonormal matrix carries the information about the direction of the divergence between the trajectories, while the upper right triangular matrix carries, mainly in its diagonal elements, the actual separation rate in each direction of the orthonormal matrix.

While conducting a numerical computation of the Lyapunov spectrum on some parameter regions unexpected jumps arise in the otherwise relatively smooth curve of the spectrum. These jumps appear specifically on simulations with a seasonal variation of a comparatively small force. The irregularities turn out to be jumps on the trajectories between coexisting attractors. We avoid these jumps between attractors by varying in the initial values of the simulations, so that we stay close to one attractor and are able to track it down from one set of initial values without jumping into neigh-

boring trajectories that happen to be on the basin of attraction of a different attractor.

The results of the seasonal variation and the Lyapunov spectra analysis have been presented and published by the author at the Conference on Computational and Mathematical Methods in Scientific Engeneering in Cádiz, Spain in 2016 [7]. These results have been also partially submitted to other publications [16].

Our study shows that the torus destruction into chaos with positive Lyapunov exponents can occur in parameter regions where also the time scale separation and hence stochastic versions of the model are possible. The chaotic motion is observed inside Arnol'd tongues of rational values of the forcing frequency and the eigenfrequency of the unforced Hopf limit cycle. Such torus bifurcations and torus destruction into chaos are also observed in other biological population systems, and were found, for example, in extended multi-strain epidemiological models on dengue fever. To understand such dynamical scenarios better also under noise, the present low dimensional system can serve as a good study case.

Chapter 1

The Rosenzweig-MacArthur Model

1.1 Preface: The Lotka Volterra System

The Lotka-Volterra equations are a system of two non linear linked differential equations of first order and they describe the interactions of populations of predators and prey. These equations were described independently by Alfred J. Lotka in 1925 and Vito Volterra in 1926. Volterra developed this model to explain the fluctuations that had been observed in the fish population in the Adriatic sea [1]. Lotka derived a similar model through the logistic equation in the theory of autocalatytic chemical reactions [8].

The equations of this model are

$$\dot{x} = \alpha x - \beta xy$$
$$\dot{y} = -\delta y + \gamma xy$$

(1.1)

where x represents a population of prey. They are assumed to have an unlimited food supply and hence reproduce at a rate α. The population of prey decreases proportional to their own population size and to the population size of predators given by y at a given rate β which represents the hunting rate of the predators.
The predators are assumed to procreate only if they have prey and at a rate γ being proportional to both populations. Finally δ represents the death rate of the predators.

The system (1.1) can be integrated directly and any solution satisfies the

conservation law

$$C = \alpha \ln y(t) - \beta y(t) - \delta x(t) + \gamma \ln x(t) \tag{1.2}$$

for a constant C and for all t.

This means that the solutions are periodic oscillations, meaning that they do not contract nor expand, which already gives some hints that this model is too simple and does not really show much resemblance with biological processes.

1.1.1   Stationary states

The ODE system (1.1) has one coexistence stationary state other than the trivial one at $x = 0$ and $y = 0$. It is given by

$$x^* = \frac{\delta}{\gamma} \tag{1.3}$$

$$y^* = \frac{\alpha}{\beta}.$$

To analyze the stability at the fixed points we first write the Jacobian matrix

$$J = \begin{pmatrix} \alpha - \beta y & -\beta x \\ \gamma y & \gamma x - \delta \end{pmatrix}. \tag{1.4}$$

At the extinction fixed point (0,0) the eigenvalues are

$$\lambda_1 = \alpha, \quad \lambda_2 = -\delta \tag{1.5}$$

which yields that the extinction point is a saddle point since α and δ are positive. This means that it is an unstable fixed point. Biologically it makes sense that the extinction point is unstable since both populations tend to aim for surviving.

At the stationary state of coexistence the eigenvalues are

$$\lambda_1 = i\sqrt{\alpha\delta}, \quad \lambda_2 = -i\sqrt{\alpha\gamma} \tag{1.6}$$

so, the sationary state is not hiperbolic. But we have seen that the solutions are closed curves that form cycles arround the stationary state.

1.1.2   Holling response functions

In order to avoid the periodic cycles that are yielded by the Lotka-Volterra model one can substitute the constant parameters with variable response functions.
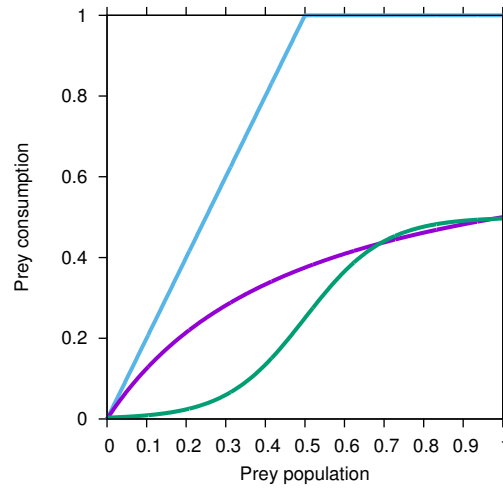
Figure 1.1: The three types of response functions as classified by Holling. Type I in blue grows linearly until it reaches a maximum and then becomes constant. Type II in lilac where the growth is descelerate with increasing number of prey. Type III in green in form of the logistic growth function.

Type I

Functional response of Type one assumes that the consuming and hunting rates are linear up to a maximum where they become constant. This type of function is used in the Lotka-Volterra model.

Type II

The type II functional response assumes that the consumption rate is descelerated with increased population explained by a limited capacity in processing food, for instance, by assuming that searching food and handling food are two separated states of the consumer.
Functions of Type II have the form

$$f(x) = \frac{cx}{d + x} \tag{1.7}$$

where x denotes some resource, food or prey.
An example of a predator prey model with Holling type II response is the Rosenzweig MacArthur model, which will be further analyzed in more detail.
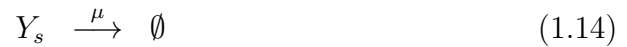
Type III

Type III functions are similar to type II, but now additionally the consumption rate is more than linear at low levels of resource. This is to be expected for instance if a population of predators first has to learn how to hunt efficiently. Holling type III response functions can be modeled with the logistic growth function

$$f(x) = \frac{L}{1 + e^{-k(x-x_0)}} \tag{1.8}$$

where L is the height of the curve, k determines the steepness and x_0 the horizontal possition of the curve.

1.2   Modelling the problem

We begin by describing the reactions of a dynamical system in population biology, where S represents an amount of resources or space and X is a population of preys that consumes said resources. Y is a population of predators which can assume two different states: Y_s are searching predators who are hungry and therefore looking for prey and Y_h are handling predators who have already satisfied their hunger and will not search for prey during this digestion state. This leads to the reaction scheme

$$S + X \ \xrightarrow{\beta} \ X + X \tag{1.9}$$
$$X \ \xrightarrow{\alpha} \ S \tag{1.10}$$
$$X + Y_s \ \xrightarrow{b} \ Y_h \tag{1.11}$$
$$Y_h \ \xrightarrow{k} \ Y_s \tag{1.12}$$
$$Y_h \ \xrightarrow{\nu} \ Y_h + Y_s \tag{1.13}$$
$$Y_s \ \xrightarrow{\mu} \ \emptyset \tag{1.14}$$
$$Y_h \ \xrightarrow{\mu} \ \emptyset \ \ . \tag{1.15}$$

Reaction (1.9) represents a prey consuming resources to procreate at a rate β. Reaction (1.10) shows preys dying at a rate α and unlocking space or resources. In reaction (1.11) we model searching predators who hunt prey and change their state to handling at a rate b. Handling predators become hungry again and change their state to searching at a rate k in reaction (1.12). Handling predators can also give birth to other predators at a rate ν, these newborn predators are assumed to be in searching state in reaction (1.13). Reaction (1.14) and (1.15) model predators dying at a rate μ.

Now we can write the differential equations that describe the changes of the system during time as

$$\dot{X} = \frac{\beta}{N}X(N-X) - \alpha X - \frac{b}{N}XY_s \qquad (1.16)$$

$$\dot{Y_h} = \frac{b}{N}XY_s - kY_h - \mu Y_h \qquad (1.17)$$

$$\dot{Y_s} = -\frac{b}{N}XY_s + kY_h - \mu Y_s + \nu Y_h \qquad (1.18)$$

where $N := X + S$ represents the maximal possible prey population, and remains constant. We can write equation (1.16) as follows

$$\dot{X} = \varrho X \left(1 - \frac{X}{\kappa}\right) - \frac{b}{N}XY_s \qquad (1.19)$$

by defining the growth rate ϱ and the carrying capacity κ by

$$\varrho := \beta - \alpha \quad \text{and} \quad \kappa := N\left(1 - \frac{\alpha}{\beta}\right)$$

as often used in ecology whereas Eq. (1.16) appears frequently in epidemiology[14].

1.3 Time Scale Separation

We consider now the processes in reactions (1.11) and (1.12) further. For many ecological studies this is a valid assuption. We can assume that the processes of predators hunting prey and handling it happen much faster than the processes of death and reproduction of preys and predators. That leads us to expect that the system of reactions (1.11) and (1.12) is almost in equilibrium in relation to the birth and death processes of reactions (1.9), (1.10), (1.13), (1.14) and (1.15).

Therefore we replace the fast variables k and b by new re-scaled variables of the order of the slow variables

$$\hat{k} := \varepsilon k \quad \text{and} \quad \hat{b} := \varepsilon b \quad .$$

We choose ε small enough to assume that the parameters $\hat{k}$ and $\hat{b}$ have the same scale as μ, ν, α and β. We now multiply equations (1.17) and (1.18) with ε and investigate the limit for $\varepsilon \to 0$ [13]. We get

$$0 = \frac{\hat{b}}{N}XY_s - \hat{k}Y_h \qquad (1.20)$$

$$0 = -\frac{\hat{b}}{N}XY_s + \hat{k}Y_h \quad . \qquad (1.21)$$

This system has a trivial equilibrium where $Y_h = 0$ and $Y_s = 0$, and another equilibrium of coexistence. To find the non-trivial fixed point define $Y :=$ $Y_s + Y_h$ as the total population of foxes and use this to get values for Y_h and Y_s as a function of X and Y as

$$Y_s = \frac{\hat{k}Y}{\hat{k} + \frac{\hat{b}}{N}X} = \frac{\varepsilon k Y}{\varepsilon k + \frac{\varepsilon b}{N}X} = \frac{kY}{k + \frac{b}{N}X} \tag{1.22}$$

$$Y_h = X\frac{Y}{\frac{\hat{k}}{\hat{b}}N + X} = X\frac{Y}{\frac{\varepsilon k}{\varepsilon b}N + X} = X\frac{Y}{\frac{k}{b}N + X} \quad . \tag{1.23}$$

We insert these values into equation (1.16) to get

$$\dot{X} = \varrho X\left(1 - \frac{X}{\kappa}\right) - k\frac{X}{\frac{k}{b}N + X}Y \tag{1.24}$$

and use (1.17) and (1.18) to find a value for $\dot{Y}$

$$\frac{d}{dt}Y = \frac{d}{dt}(Y_s + Y_h) = -\mu(Y_s + Y_h) + \nu Y_h = -\mu Y + \nu X\frac{Y}{\frac{k}{b}N + X} \quad . \tag{1.25}$$

This leads us to the system of a Rosenzweig-MacArthur type model with Holling type II response function

$$\begin{aligned}\dot{X} &= \varrho X\left(1 - \frac{X}{\kappa}\right) - k\frac{X}{\frac{k}{b}N + X}Y \\ \dot{Y} &= -\mu Y + \nu\frac{X}{\frac{k}{b}N + X}Y \quad .\end{aligned} \tag{1.26}$$

This system will later be compared to the system of equations (1.16), (1.17) and (1.18).

We calculate its stationary state of coexistence, apart from the two trivial fixed points $X^* = Y^* = 0$ and $Y^* = 0$, $X^* = \kappa$, and obtain

$$X^* = \frac{\mu\frac{k}{b}N}{\nu - \mu} \tag{1.27}$$

$$Y^* = \frac{\nu}{k}\varrho\frac{Nk}{b(\nu - \mu)}\left(1 - \frac{\mu\frac{k}{b}N}{\kappa(\nu - \mu)}\right) \quad . \tag{1.28}$$

For simplification we define $\varphi(X) := \frac{X}{\frac{k}{b}N + X}$. Note that $\varphi(X^*) = \frac{\mu}{\nu}$. Using this function we can write the Jacobi Matrix of the stationary state as follows

$$A = \begin{pmatrix} \varrho\left(1 - \frac{X^*}{\kappa}\right) - \varrho\frac{X^*}{\kappa} - k\varphi'(X^*)Y^* & -\frac{k}{\nu}\mu \\ \nu\varphi'(X^*)Y^* & 0 \end{pmatrix} \quad . \tag{1.29}$$

Again for further simplification we define

$$\tilde{a} := \varrho \left(1 - \frac{X}{\kappa}\right) - \varrho\frac{X}{\kappa} \quad \text{and} \quad \tilde{b} := \nu\varphi'(X)Y \quad,$$

and write the Jacobi Matrix in a simpler form

$$A = \begin{pmatrix} \tilde{a} - \frac{\kappa}{\mu}\tilde{b} & -\frac{\kappa}{\nu}\mu \\ \tilde{b} & 0 \end{pmatrix} \tag{1.30}$$

to calculate the eigenvalues

$$\lambda_{1/2} = \frac{\tilde{a} - \frac{k}{\nu}\tilde{b} \pm \sqrt{\left(\tilde{a} - \frac{k}{\nu}\tilde{b}\right)^2 - 4\tilde{b}\frac{k}{\nu}\mu}}{2} \quad. \tag{1.31}$$

A Hopf bifurcation arises when the eigenvalues of the Jacobi Matrix cross the imaginary axis because of a variation of the parameters. Here we can see that this system has a Hopf bifurcation point for $\tilde{a} - \frac{k}{\nu}\tilde{b} = 0$, i.e. a point where we have only a rotational part via the imaginary unit from the square root with negative argument, but no contraction or expansion from the real part of the eigenvalues. If $\tilde{a} - \frac{k}{\nu}\tilde{b} = 0$ then the eigenvalues are purely imaginary, if $\tilde{a} - \frac{k}{\nu}\tilde{b} < 0$ then the real part of the eigenvalues is negative and for $\tilde{a} - \frac{k}{\nu}\tilde{b} > 0$ the real part of the the two eigenvalues will be positive. When changing relevant parameters the slope is non vanishing at the bifurcation point.

Inserting the designated values for $\tilde{a}$ and $\tilde{b}$ and solving for ν gives

$$\nu_H = \frac{\frac{\kappa}{N} + \frac{\kappa}{b}}{\frac{\kappa}{N} - \frac{\kappa}{b}} \cdot \mu \tag{1.32}$$

as the value ν_H of the parameter ν at which the Hopf bifurcation happens.

1.4 Stationary States and Stability Analysis

Let us define $Z := Y_s$ in order to write our differential equations system in the following form

$$\dot{X} = \varrho X \left(1 - \frac{X}{\kappa}\right) - \frac{b}{N}XZ \tag{1.33}$$

$$\dot{Y} = (\nu - \mu)Y - \nu Z \tag{1.34}$$

$$\dot{Z} = \frac{b}{N}XZ + (k + \nu)(Y - Z) - \mu Z \quad. \tag{1.35}$$

We incorporate the total number of prey units and the total number of predators, and needing a third degree of freedom we use $Z := Y_s$. In this form we can easily consider a two dimensional reduced system of states X and Y in a Rosenzweig-MacArthur model as well as the original extended system with the searching and handling process explicitly included. We will first investigate the reduced system and use the results from its fixed point and stability analysis to then understand the behavior of the extended system.

1.4.1 Two Dimensional Reduced System

First consider a time scale separation of equation (1.35). This leads us to analyze Z as a function of X and Y

$$Z(X,Y) = \frac{\hat{k}}{\hat{k} + \frac{\hat{b}}{N}X}Y = \frac{k}{k + \frac{b}{N}X}Y. \tag{1.36}$$

Since $\hat{k} = \varepsilon k$ and $\hat{b} = \varepsilon b$ we can cancel the epsilons and work with k and b instead of $\hat{k}$ and $\hat{b}$. Now we have the following two dimensional system

$$\dot{X} = \varrho X\left(1 - \frac{X}{\kappa}\right) - \frac{b}{N}XZ(X,Y) \tag{1.37}$$

$$\dot{Y} = (\nu - \mu)Y - \nu Z(X,Y) \quad . \tag{1.38}$$

Apart from the trivial ones, it has stationary states at

$$X_a^* = \frac{\mu}{\nu - \mu} \cdot \frac{k}{b}N \tag{1.39}$$

$$Y_a^* = \frac{\nu}{\nu - \mu} \cdot \frac{\varrho}{b}\left(1 - \frac{\nu}{\nu - \mu} \cdot \frac{k}{b} \cdot \frac{N}{\kappa}\right)N \quad . \tag{1.40}$$

From the condition $Y_a^* = 0$, where the stationary state of coexistence meets the stationary state of extinction, we obtain the value of ν of the transcritical bifurcation as

$$\nu_{transcritical} = \left(1 + \frac{k}{b} \cdot \frac{N}{\kappa}\right) \quad . \tag{1.41}$$

With the Jacobian matrix

$$A = \begin{pmatrix} \varrho\frac{\mu}{\nu} - \varrho\left(1 + \frac{\mu}{\nu}\right)\frac{X_a^*}{\kappa} & -\frac{1}{\varepsilon}\hat{k}\frac{\mu}{\nu} \\ \varepsilon(\mu - \nu)\frac{\varrho}{k}\left(1 - \frac{X_a^*}{\kappa}\right) & 0 \end{pmatrix} = \begin{pmatrix} a_{11} & a_{12} \\ a_{21} & a_{22} \end{pmatrix}. \tag{1.42}$$

The eigenvalues are of the form

$$(\lambda_a)_{1/2} = \underbrace{\frac{1}{2}a_{11}}_{r_a} \pm \underbrace{\sqrt{\frac{1}{4}a_{11}^2 - a_{12}a_{21}}}_{\omega_a} \qquad (1.43)$$

and were already explicitly given in equation (1.31). This gives the basis of the system in terms of its bifurcations, and most of it can be used in the understanding of the extended system.

1.4.2 Three Dimensional Extended System

The original three dimensional system of equations (1.33), (1.34), (1.35), has a stationary state of coexistence at

$$X_b^* = \frac{\mu}{\nu - \mu}\frac{kb}{N} + \nu - \mu\left(\frac{\nu}{\nu - \mu}\right) = X_a^* + \varepsilon\frac{\mu}{\nu - \mu}\frac{\mu}{\hat{b}}N \qquad (1.44)$$

$$Y_b^* = \varrho\frac{N}{b}\frac{\nu}{\nu - \mu}\left(1 + \frac{\mu(\mu + k)}{\kappa(\nu - \mu)}\right) \qquad (1.45)$$

$$Z_b^* = \varrho\frac{N}{b}\left(1 + \frac{\mu(\mu + k)}{\kappa(\nu - \mu)}\right) \qquad (1.46)$$

and its Jacobi matrix is

$$B = \begin{pmatrix} -\varrho\frac{X_b^*}{\kappa} & 0 & -\frac{b}{N}X_b^* \\ 0 & \nu - \mu & -\nu \\ -\varrho\left(1 - \frac{X_b^*}{\kappa}\right) & k + \nu & -\frac{b}{N}X_b^* - (k + \nu) - \mu \end{pmatrix} =: \begin{pmatrix} b_{11} & 0 & b_{13} \\ 0 & b_{22} & b_{23} \\ b_{31} & b_{32} & b_{33} \end{pmatrix}.$$

The eigenvalues are the solutions of the characteristic polynomial

$$0 = |B - \lambda\mathbb{1}| = -\lambda^3 + \underbrace{(b_{11} + b_{22} + b_{33})}_{=:b_2}\lambda^2$$

$$+ \underbrace{(-b_{11}b_{22} - b_{11}b_{33} - b_{22}b_{23} + b_{31}b13 + b_{32}b_{23})}_{=:b_1}\lambda \qquad (1.47)$$

$$+ \underbrace{b_{11}b_{22}b_{23} - b_{31}b_{22}b_{13} - b_{32}b_{23}b_{11}}_{=:b_0}$$

$$= -\lambda^3 + b_2\lambda^2 + b_1\lambda + b_0 \quad .$$

Now let us assume that the rotational behavior is similar to the one in the reduced two dimensional system. That means that we can expect two eigenvalues to have complex values close to the eigenvalues of the reduced system

and the third eigenvalue would have a real value to be largely negative, as it turns out of order of $\frac{1}{\varepsilon}$

$$(\lambda_b)_{1/2} = \underbrace{r_b}_{r_a + \varepsilon q} \pm i \underbrace{\omega_b}_{\omega_a + \varepsilon \omega} \quad , \qquad \lambda_{b3} = c. \tag{1.48}$$

We evaluate the characteristic polynomial for these values and obtain

$$-\lambda^3 + \underbrace{(2r_b + c)}_{b_2} \lambda^2 + (-2cr_b - r_b^2 - \omega_b^2)\lambda + cr_b^2 + c\omega^2 = 0 \quad . \tag{1.49}$$

Now we use $2r_b + c = b_2$ to find c as

$$c = b_{11} + b_{22} + b_{33} - 2(r_a + \varepsilon q) \tag{1.50}$$

$$\Rightarrow \lambda_3 = \lambda^{\left(\frac{1}{\epsilon}\right)} + \lambda^{(1)} + \mathcal{O}(\varepsilon) \tag{1.51}$$

with eigenvalue parts of order $(1/\varepsilon)$, hence $\lambda^{\left(\frac{1}{\varepsilon}\right)}$, and of order 1, hence $\lambda^{(1)}$ given by

$$\lambda^{\left(\frac{1}{\epsilon}\right)} = -\frac{1}{\epsilon} \left(\frac{\hat{b}}{N} X_a^* + \hat{k} \right) \tag{1.52}$$

$$\lambda^{(1)} = -\varrho \frac{X_a^*}{\kappa} + \nu - \mu - \left(\hat{b} \frac{\mu N}{(\nu - \mu)\hat{b}} + \nu + \mu \right)$$
$$+ \frac{\mu}{\nu - \mu}(\mu - 2\nu) - \varrho \frac{\mu}{\nu} \left(1 - \frac{\mu k N}{(\mu + \nu)b\kappa} \right) \quad . \tag{1.53}$$

These values were confirmed numerically by simulations.

This finishes the analysis of the deterministic dynamical system. Now we will use the results from above to construct a stochastic system with a Hopf bifurcation corresponding to the one we just saw in the deterministic model.

1.5 Simulation

For the model to fulfill a time scale separation we asign values to the parameters that conform an ecological model. In this sense the preys have a lifespan of roughly half a year, so $\alpha := \frac{1}{\frac{1y}{2}} = 2y^{-1}$. Assuming they procreate fast gives $\beta := 20\alpha$. We assume that the predators have a lifespan of 10 months and a procreation rate twice as fast as the mortality, so $\mu := \frac{1}{\frac{10y}{12}} = \frac{6}{5}y^{-1}$ and $\nu := 2\mu$. Further, the predators would have a digestion rate of 1 day, hence $k := \frac{1}{1d} = 365y^{-1}$. And varying the predator hunting rate.
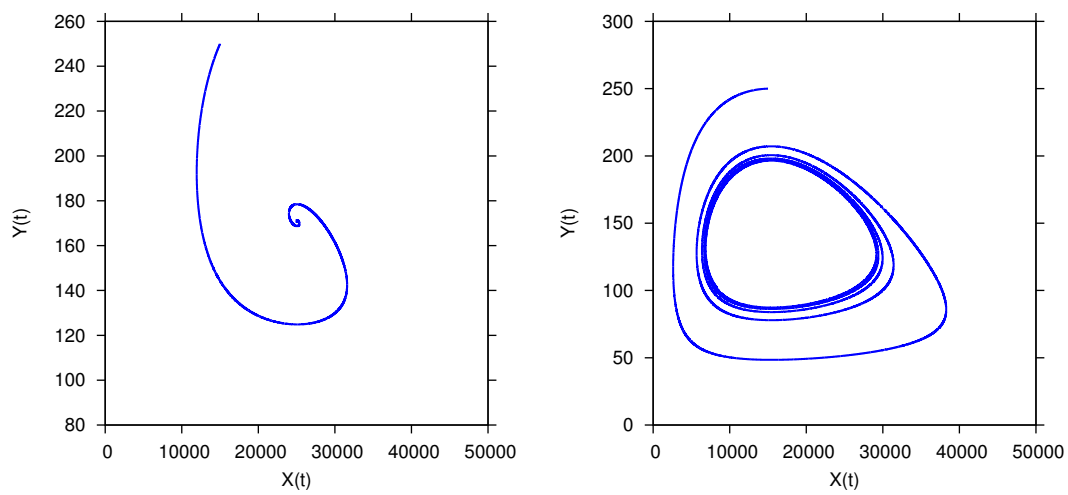
Figure 1.2: Spiraling into a fixpoint for $b = 2k$, on the left side, and into a limit cycle for $b = 6.5k$.

Chapter 2

Master Equation and Fokker-Planck Equation

2.1 Master Equation

Generally speaking, the master equation is derived as the differential of the Chapman-Kolmogorov equation for Markovian stochastic processes[11]. Its name is derived from a paper of A. Nordsieck et. al. from 1940 in which it had the role of a general equation from which all the other results were derived [9]. The master equation can be interpreted as a gain-loss equation for the probabilities of separate states. We use this more intuitive interpretation to derive the master equation for our model.

Keeping in mind our definitions of $Y = Y_h + Y_s$ and $Z = Y_s$, we can write the reaction scheme as a stochastic process in terms of a master equation [14, 11, 2] of our system in dependency of X, Y and Z. For $\underline{n} = (X, Y, Z)^{tr}$ (using the underbar notation $\underline{n}$ for a vector and $\underline{n}^{tr}$ for its transpose) we have the master equation as time evolution equation of the probabilities to find the state $\underline{n}$ at time t given by

$$\frac{d}{dt} p(\underline{n}) = \sum_{\tilde{\underline{n}} \neq \underline{n}} w_{\underline{n},\tilde{\underline{n}}} p(\tilde{\underline{n}}) - \sum_{\tilde{\underline{n}} \neq \underline{n}} w_{\tilde{\underline{n}},\underline{n}} p(\underline{n}) \quad . \tag{2.1}$$

We can restrain to the $\tilde{\underline{n}}$ that only differ on one of the three components by 1 from $\underline{n}$, due to the limit of small transition probability changes in small
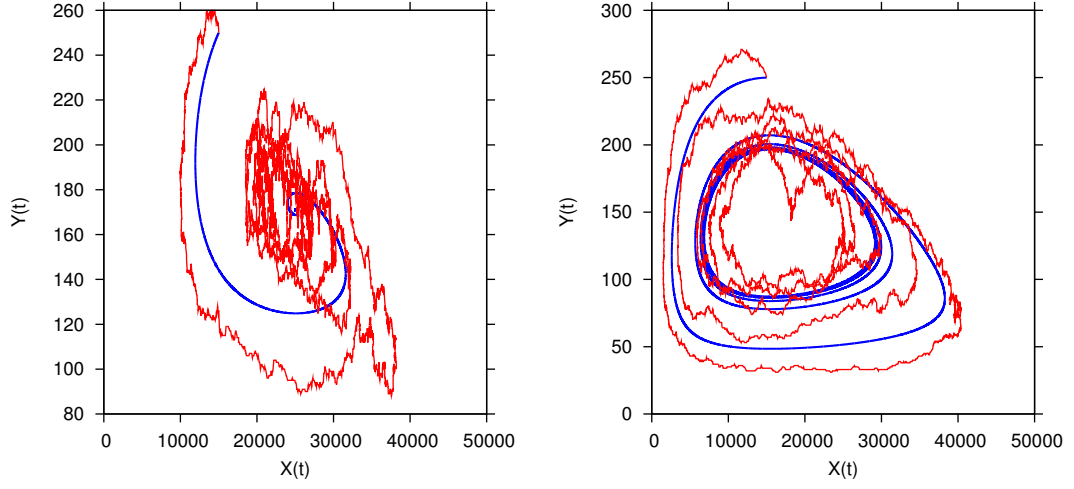
21

Figure 2.1: Spiraling into a fix point on the left and into the limit cycle on the right, starting from arbitrary initial conditions of stochastic and deterministic system in comparison. The parameters are set as in Section 1.5 throughout this chapter.

time steps Δt, obaining

$$
\begin{aligned}
\frac{d}{dt}p(X,Y,Z) =& \frac{\beta}{N}(N - (X - 1))(X - 1)p(X - 1, Y, Z) \\
& + \alpha(X + 1)p(X + 1, Y, Z) \\
& + \frac{b}{N}(X + 1)(Z + 1)p(X + 1, Y, Z + 1) \\
& + k(Y - Z + 1)p(X, Y, Z - 1) \\
& + \nu(Y - Z)p(X, Y - 1, Z - 1) \\
& + \mu(Z + 1)p(X, Y + 1, Z + 1) \\
& + \mu(Y - Z + 1)p(X, Y + 1, Z) \\
& - \left(\frac{\beta}{N}(N - X)X + \alpha X + \frac{b}{N}XZ + k(Y - Z) \right. \\
& \left. + \nu(Y - Z) + \mu Z + \mu(Y - Z) \right) p(X, Y, Z) \quad .
\end{aligned}
\tag{2.2}
$$

Using Gillespie's algorithm [3, 4] with exponential waiting times between jumps of states, we can simulate stochastic realizations of the process XYZ and compare with the deterministic version of the model given by the ODE system, equations (1.33) to (1.35), see figure 2.1. We start with initial conditions outside the expected limit cycle for $b = 6.5 \cdot k$ and oscillate into the limit

cycle, once we passed the Hopf bifurcation point. The stochastic realization plotted here fluctuates well around the mean field curve.

However, in systems with large population size N the simulation of the master equation becomes very slow, due to large numbers of transitions in small time intervals, and approximation methods are desired. Hence we reformulate the master equation in densities $x := X/N$, $y := Y/N$ and $z := Z/N$ and then can use Taylor's expansion in $1/N$ to obtain a Fokker-Planck equation giving a stochastic differential equation (SDE) system. This SDE system is much faster in simulations, since it does not depend explicitly on simulation steps proportional to the system size.

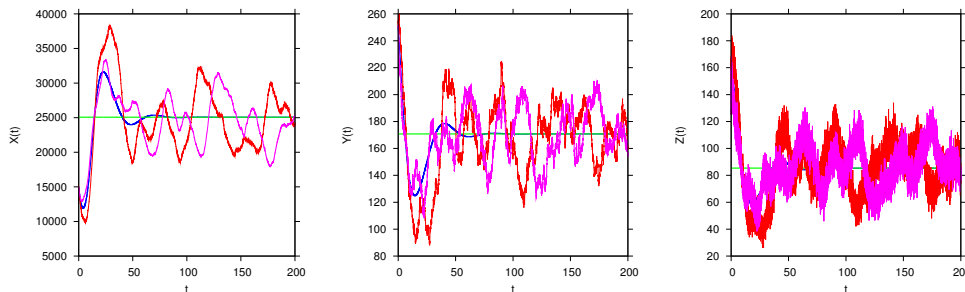## 2.2 From Master Equation to Fokker-Planck Equation

Figure 2.2: Time series plot for the prey population $X(t)$, the total number of predators $Y(t)$ and the searching predators $Z(t) = Y_s(t)$. Fluctuations around the fix point in green, the deterministic system in blue, the Master Equation approach in red and the Fokker-Planck appraoch in pink.

The Fokker-Planck equation is a special kind of master equation which is often used as an approximation to the actual equation[11]. We will derive the Fokker-Planck equation by conducting a Taylor's transformation on the transition probabily from a density state to a neighboring state.

With densities $x := X/N$, $y := Y/N$ and $z := Z/N$ we get the master

equation

$$
\begin{aligned}
\frac{d}{dt}p(x,y,z,t) = \; & N\beta\left(1-\left(x-\frac{1}{N}\right)\right)\left(x-\frac{1}{N}\right)p\left(x-\frac{1}{N},y,z,t\right) \\
& + N\alpha\left(x+\frac{1}{N}\right)p\left(x+\frac{1}{N},y,z,t\right) \\
& + Nb\left(x+\frac{1}{N}\right)\left(z+\frac{1}{N}\right)p\left(x+\frac{1}{N},y,z+\frac{1}{N},t\right) \\
& + Nk\left(y-z+\frac{1}{N}\right)p\left(x,y,z-\frac{1}{N},t\right) \\
& + N\nu\,(y-z)\,p\left(x,y-\frac{1}{N},z-\frac{1}{N},t\right) \\
& + N\mu\left(z+\frac{1}{N}\right)p\left(x,y+\frac{1}{N},z+\frac{1}{N},t\right) \\
& + N\mu\left(y-z+\frac{1}{N}\right)p\left(x,y+\frac{1}{N},z,t\right) \\
& - \Big(N\beta\,(1-x)\,x + N\alpha x + Nbxz + Nk\,(y-z) \\
& \quad\; + N\nu\,(y-z) + N\mu z + N\mu\,(y-z)\Big)\,p\,(x,y,z,t) \qquad .
\end{aligned}
\tag{2.3}
$$

with $\underline{x} := (x,y,z)^{tr}$ as state vector and for the seven transitions $w_j(\underline{x})$ and vectors of small changes $\Delta\underline{x}_j := \frac{1}{N}\cdot\underline{r}_j$, with

$$
\underline{r}_1 = \begin{pmatrix} -1 \\ 0 \\ 0 \end{pmatrix}, \qquad
\underline{r}_2 = \begin{pmatrix} 1 \\ 0 \\ 0 \end{pmatrix}, \qquad
\underline{r}_3 = \begin{pmatrix} 1 \\ 0 \\ 1 \end{pmatrix}, \qquad
\underline{r}_4 = \begin{pmatrix} 0 \\ 0 \\ -1 \end{pmatrix},
$$

$$
\underline{r}_5 = \begin{pmatrix} 0 \\ -1 \\ -1 \end{pmatrix}, \qquad
\underline{r}_6 = \begin{pmatrix} 0 \\ 1 \\ 1 \end{pmatrix}, \qquad
\underline{r}_7 = \begin{pmatrix} 0 \\ 1 \\ 0 \end{pmatrix}.
$$

Then the master equation, Eq. (2.3), can be written in the easily generalizable form for $n = 7$ transitions

$$
\frac{d}{dt}\,p(\underline{x},t) = \sum_{j=1}^{n}\Big(\,Nw_j(\underline{x}+\Delta\underline{x}_j)\cdot p(\underline{x}+\Delta\underline{x}_j,t)\; - Nw_j(\underline{x})\cdot p(\underline{x},t)\Big)
\tag{2.4}
$$

and with the gradient vector

$$
\nabla_{\underline{x}} = \begin{pmatrix} \frac{\partial}{\partial x} \\ \frac{\partial}{\partial y} \\ \frac{\partial}{\partial z} \end{pmatrix} = \partial_{\underline{x}}
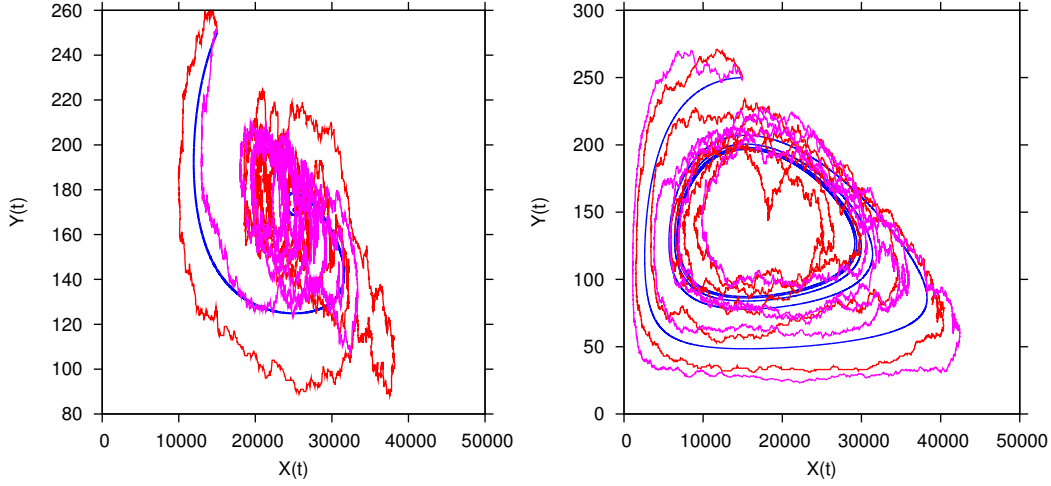\tag{2.5}
$$

Figure 2.3: Spiraling into a fixpoint for $b = 2k$, on the left side, and into a limit cycle for $b = 6.5k$ on the right side. The deterministic system in blue, the Master Equation approach in red and the Fokker Planck equation in pink.

using the interchangable notations $\nabla_{\underline{x}}$ or $\partial_{\underline{x}}$ in the following. Taylor's expansion gives

$$w_j(\underline{x} + \Delta\underline{x}_j) \cdot p(\underline{x} + \Delta\underline{x}_j, t) = \sum_{\nu=0}^{\infty} \frac{1}{\nu!} \left(\Delta\underline{x}_j \cdot \nabla_{\underline{x}} \right)^{\nu} w_j(\underline{x}) \, p(\underline{x}, t) \qquad (2.6)$$

and to second order applied to the master equation, Eq. (2.4), we obtain the following Fokker-Planck equation

$$\frac{\partial}{\partial t} \, p(\underline{x}, t) = -\nabla_{\underline{x}} \left(\sum_{j=1}^{n} (-\underline{r}_j \cdot w_j(\underline{x})) \, p(\underline{x}, t) \right) + \frac{\sigma^2}{2} \sum_{j=1}^{n} (\underline{r}_j \cdot \nabla_{\underline{x}})^2 w_j(\underline{x}) \, p(\underline{x}, t)$$

$$(2.7)$$

or in different notation

$$\frac{\partial}{\partial t} \, p(\underline{x}, t) = -\partial_{\underline{x}} \left(\underline{f}(\underline{x}) \, p(\underline{x}, t) \right) + \frac{\sigma^2}{2} \, \overrightarrow{\partial_{\underline{x}}} \left(G^2(\underline{x}) \, p(\underline{x}, t) \right) \overleftarrow{\partial_{\underline{x}}} \qquad . \qquad (2.8)$$

Here the expression $\overrightarrow{\partial_{\underline{x}}} \left(G^2(\underline{x}) \, p(\underline{x}, t) \right) \overleftarrow{\partial_{\underline{x}}}$ is simply a quadratic form, for the

XYZ system being explicitly

$$\left(\frac{\partial}{\partial x}, \frac{\partial}{\partial y}, \frac{\partial}{\partial z} \right) \cdot \left(\begin{array}{ccc} g_{11} & g_{12} & g_{13} \\ g_{21} & g_{22} & g_{23} \\ g_{31} & g_{32} & g_{33} \end{array} \right)^2 p(\underline{x}, t) \cdot \left(\begin{array}{c} \overleftarrow{\frac{\partial}{\partial x}} \\[1ex] \overleftarrow{\frac{\partial}{\partial y}} \\[1ex] \overleftarrow{\frac{\partial}{\partial z}} \end{array} \right) . \tag{2.9}$$

The partial derivatives are acting to the right respectively to the left around the matrix $G^2 p$, which is indicated by the arrows on the gradients, $\overrightarrow{\partial_{\underline{x}}}$ and $\overleftarrow{\partial_{\underline{x}}}$, in Eq. (2.8). Hence for the vector in the drift term $\underline{f}(\underline{x})$ and the matrix of the diffusion term $G^2(\underline{x})$ we have the explicit form from the transitions $w_j(\underline{x})$

$$\underline{f}(\underline{x}) = \sum_{j=1}^{n} \underline{f}_j(\underline{x}) = \sum_{j=1}^{n} (-\underline{r}_j \cdot w_j(\underline{x})) \tag{2.10}$$

and

$$G^2(\underline{x}) = \sum_{j=1}^{n} G_j^2(\underline{x}) = \sum_{j=1}^{n} \underline{r}_j \cdot \underline{r}_j^{tr} \, w_j(\underline{x}) \tag{2.11}$$

with in the case of the XYZ system the three dimensional matrix

$$\underline{r}_j \cdot \underline{r}_j^{tr} = \left(\begin{array}{c} r_x \\ r_y \\ r_z \end{array} \right) \cdot (r_x, r_y, r_z) = \left(\begin{array}{ccc} r_x^2 & r_x \cdot r_y & r_x \cdot r_z \\ r_x \cdot r_y & r_y^2 & r_y \cdot r_z \\ r_x \cdot r_z & r_y \cdot r_z & r_z^2 \end{array} \right) \tag{2.12}$$

this matrix is always symmetric, also in more general cases. This allows easily to take the matrix square root $G(\underline{x}) = T\sqrt{\Lambda} T^{tr}$ from the decomposition $G^2(\underline{x}) = T\Lambda T^{-1}$. Corresponding to the Fokker-Planck equation we obtain the stochastic differential equation system

$$\frac{d}{dt} \underline{x} = \underline{f}(\underline{x}) + \sigma G(\underline{x}) \cdot \underline{\varepsilon}(t) \tag{2.13}$$

with $\sigma = 1/\sqrt{N}$ and in the XYZ case the three dimensional Gaussian normal noise vector $\underline{\varepsilon}(t) = (\varepsilon_x(t), \varepsilon_y(t), \varepsilon_z(t))^{tr}$.

Chapter 3

Seasonal Forcing and Torus Bifurcation

3.1 Seasonal Forcing of the Predator Birth Rate

We recall the Rosenzweig-MacArthur model with Holling type II response function

$$
\begin{aligned}
\dot{X} &= \varrho X \left(1 - \frac{X}{\kappa}\right) - k \frac{X}{\frac{k}{b}N + X} Y \\
\dot{Y} &= -\mu Y + \nu \frac{X}{\frac{k}{b}N + X} Y \quad .
\end{aligned}
\tag{3.1}
$$

Now, we want to implement seasonal variation on the predator birth rate. For this we define a new predator birth rate $\nu(t)$ dependet on the time with a cosinusoidal variation around a mean predator birth rate ν_0, hence

$$
\nu = \nu(t) = \nu_0(1 + \mu \cos(\omega(t + \phi)))
\tag{3.2}
$$

with frequency $\omega = 2\pi \frac{1}{T}$ and period $T = 1 year$. The phase offset ϕ is useful to describe models where the birth rate is maximal in the summer on a time scale given in years, for our theoretical study it is not needed. Hence we can assume perfect cosinusoidal forcing and set $\phi = 0$. We get the seasonally forced system with forced parameter $\nu(t)$

$$
\begin{aligned}
\dot{X} &= \varrho X \left(1 - \frac{X}{\kappa}\right) - k \frac{X}{\frac{k}{b}N + X} Y \\
\dot{Y} &= -\mu Y + \nu(t) \frac{X}{\frac{k}{b}N + X} Y \\
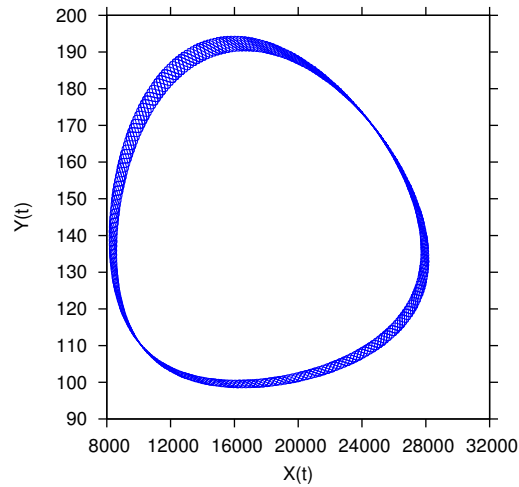\nu(t) &= \nu_0(1 + \eta cos(\omega t))
\end{aligned}
\tag{3.3}
$$

Figure 3.1: A torus trajectory for the seasonally forced system. Transients are cut off to show the final atractor.

This is, however, a non-autonomous system, and in order to keep the classification of limit cycles, tori and others, an autonomous system is needed. So, we have to transform the seasonally forced, non-autonomous system into an autonomous system. This is achieved by implementing additional dimensions given by an oscillator.

3.2 Autonomous System via Hopf Oscillator

We use here a Hopf oscillator with a stable sinusoidal limit cycle instead of a most commonly used harmonic oscillator in order to avoid jumping between trajectories when varying initial conditions. The equations of the Hopf oscillator are

$$\begin{aligned} \dot{x} &= -\omega y + cx(\eta^2 - (x^2 + y^2)) \\ \dot{y} &= \omega x + cy(\eta^2 - (x^2 + y^2)) \end{aligned} \quad . \tag{3.4}$$

If we choose appropiate initial conditions, in this case $x(t_0) = \eta$, $y(t_0) = 0$ [16], the solution of the Hopf oscillator is

$$x(t) = \eta cos(\omega t) \quad .$$

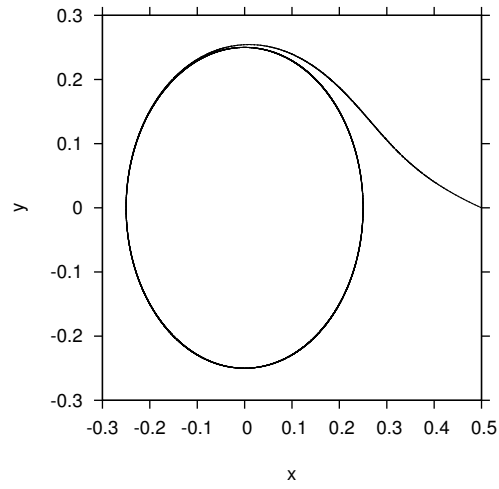Coupling the whole system with the Hopf oscillator yields

Figure 3.2: A Hopf oscillator converges into a stable sinusoidal limit cycle, making it more stable to numerical errors than the harmonic oscillator.

$$\dot{X} = \varrho X \left(1 - \frac{X}{\kappa}\right) - k\frac{X}{\frac{k}{b}N + X}Y$$
$$\dot{Y} = -\mu Y + \nu_0(1 + x)\frac{X}{\frac{k}{b}N + X}Y \qquad (3.5)$$
$$\dot{x} = -\omega y + cx(\eta^2 - (x^2 + y^2))$$
$$\dot{y} = \omega x + cy(\eta^2 - (x^2 + y^2))$$

Chapter 4

Lyapunov Spectra Analysis

The Lyapunov spectrum of a dynamichal system is the set of Lyapunov exponents of the system. Lyapunov exponents give a quantification of the separation of neighboring initial states. Hence when all Lyapunov exponents are negative, the trajectories starting from neighboring initial conditions are getting closer with the time, e.g. limit cycles appear. If the biggest Lyapunov exponent is equal to zero, then a bifurcation is occuring. And if at least one of the exponents is positive, the dynamics of the system are chaotic.

Lyapunov exponents are defined as the real part of the eigenvalues on the fixpoints of a system. On limit cycles, they are defined as the real part of the Floquet multipliers.

An effective way to compute the Lyapunov spectrum is by first conducting a QR-decomposition on a sequence of Jacobian matrices along points on an orbit. Then adding up the logarithms of the diagonal entries of the upper right triangular matrix R [10].

4.1   Jacobian Matrices

In order to calculate the Lyapunov exponents of the forced Rosenzweig-MacArthur system and the autonomous four-dimensional system, we compute first the respective Jacobian matrices.

Recall the definition of φ stated while conducting the stability analysis of the reduced two-dimensional model

$$\varphi = \frac{X}{\frac{k}{b}N + X} \quad . \tag{4.1}$$

The Jacobian matrix for the two-dimensional forced Rosenzweig-MacArthur system is then

$$A = \begin{pmatrix} \varrho \left(1 - 2\frac{X}{\kappa}\right) - k\varphi\prime(X)Y & -k\varphi(X) \\ \nu(t)\varphi\prime(X)Y & -\mu + \nu(t)\varphi(X) \end{pmatrix} \qquad (4.2)$$

and for the autonomous four-dimensional system

$$B = \begin{pmatrix} \varrho \left(1 - 2\frac{X}{\kappa}\right) - k\varphi\prime(X)Y & -k\varphi(X) & 0 & 0 \\ \nu(t)\varphi\prime(X)Y & -\mu + \nu_0(1+x)\varphi(X) & \nu_0\varphi(X)Y & 0 \\ 0 & 0 & c(\eta^2 - (x^2 + y^2)) - 2cx^2 & -\omega - 2cxy \\ 0 & 0 & \omega - 2cxy & c(\eta^2 - (x^2 + y^2)) - 2cx^2 \end{pmatrix} \qquad (4.3)$$

4.2 Computation of the Lyapunov Spectrum

Now that we have the expression of the Jacobian matrices Df we can compute them at a series points x^i along an orbit. We look at N_t iterations along an orbit, each at a time step of Δt. For the computation we set $\Delta t = 10^{-3}$. We have the product of the N_t Jacobian matrices

$$Df^{N_t} := \prod_{i=1}^{N_t} = Df(x^{N_t}) \cdot Df(x^{N_t-1}) \cdot ... \cdot Df(x^2) \cdot Df(x^1) \quad . \qquad (4.4)$$

We start by decomposing the first Jacobian matrix $Df(x^1)$ into a orthonormal matrix Q^1 and an upper right triangular matrix R^1 and get

$$Df^{N_t} = Df(x^{N_t}) \cdot Df(x^{N_t-1}) \cdot ... \cdot Df(x^2) \cdot Q^1 \cdot R^1 \quad . \qquad (4.5)$$

Now we decompose the matrix $Df(x^2) \cdot Q^1$ into another orthonormal matrix Q^2 and an upper right triangular matrix R^2

$$Df^{N_t} = Df(x^{N_t}) \cdot Df(x^{N_t-1}) \cdot ... \cdot Q^2 \cdot R^2 \cdot R^1 \quad . \qquad (4.6)$$

We repeat this decomposition of the product of the Jacobian matrix at the time step i $Df(x^i)$ with the orthogonal matrix Q^{i-1} at the previous step. At the end we get

$$Df^{N_t} = Q^{N_t} \cdot R^{N_t} \cdot R^{N_t-1} \cdot ... \cdot R^2 \cdot R^1 \quad . \qquad (4.7)$$

Geometrically speaking, this matrix carries the information about the deviation from neighboring states after N_t timesteps of size t. Also, solely the orthogonal matrix Q^{N-t} carries all the information about the direction of

said deviations. The information about the length of these deviations is carried in the product of the upper triangular matrices $\prod_{i=0}^{N_t} R^i$.

This information is best coded into the Lyapunov exponents λ_k given as

$$\lambda_k = \lim_{N_t \to \infty} \frac{1}{N \Delta t} \ln \prod_{i=1}^{N} r_{kk}^i = \lim_{N_t \to \infty} \frac{1}{N \Delta t} \sum_{i=1}^{N} \ln r_{kk}^i \quad . \tag{4.8}$$

Where r_{kk}^i are the diagonal entries of the triangular matrix R^i.

4.3 Parameters used in previous studies
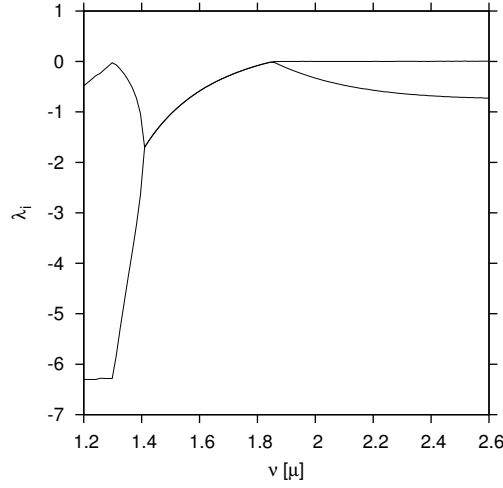
Figure 4.1: Lyapunov spectrum of the unforced Rosenzweig-MacArthur model with parameters as set by Rinaldi et al. with a transcritical point at $\nu = 1.3\mu$ given by both eigenvalues of the Jacobian matrix becoming complex conjugated and having identical real part. And a Hopf bifurcation point at $\nu = 1.85714\mu$ given by both eigenvalues of the Jacobian matrix becoming zero and after the bifurcation point one of the eigenvalues stays zero and the other becomes negative.

In 1993, an analysis of the chaotic behaviour of predator prey systems was conducted by Rinaldi, Muratori and Kuznetsov [12]. There, the following parameters were given for the Rosenzweig-MacArthur model with Holling type II response function with lumped parameters $\tilde{a}$ and $\tilde{b}$ e.g.

$$\dot{X} = \tilde{r}X \left(1 - \frac{X}{\tilde{k}} \right) - \frac{\tilde{a}X}{\tilde{b} + X} Y$$

$$\dot{Y} = -\tilde{d}Y + \tilde{e} \frac{\tilde{a}X}{\tilde{b} + X} Y \tag{4.9}$$

with the default parameters given as $\tilde{k} = \tilde{e} = 1$, $\tilde{r} = \tilde{d} = 2\pi$, $\tilde{a} = 2 \cdot 2\pi$ and $\tilde{b} = 0.3$. Hence in comparison with our notation we have from these lumped parameters $\varrho = \tilde{r} = 2\pi$, $\kappa = \tilde{k} = 1$, $k = \tilde{a} = 2 \cdot 2\pi$, $b = \frac{\tilde{a}}{\tilde{b}} \cdot N = \frac{2 \cdot 2\pi}{0.3} \cdot N$ with $N = 1$ by default, $\mu = d = 2\pi$ and $\nu = \tilde{e} \cdot \tilde{a} = 2 \cdot 2\pi$.
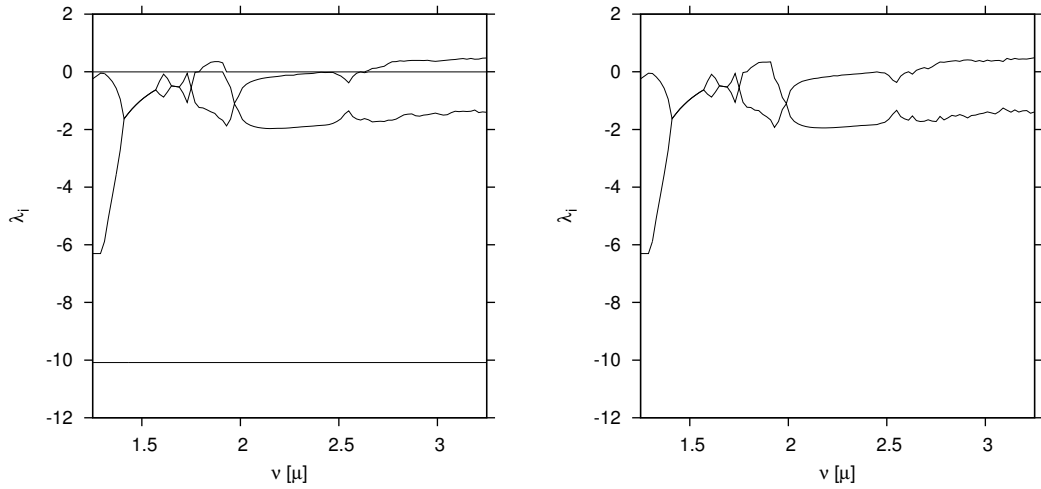
4.4   Numerical Computation

Figure 4.2: On the left: Lyapunov spectrum of the 4-dimensional autonomous system of the Rosenzweig-MacArthur coupled with a Hopf oscillator showing the two trivial Lyapunov exponents zero and $2c\eta = -10$ as well as the non-trivial Lyapunov exponents. On the right: Lyapunov spectrum of the forced 2-dimensional Rosenzweig-MacArthur model showing only the two non-trivial Lyapunov exponents.

The Lyapunov exponents of the Hopf oscillator can be calculated analytically [16]. For the system of the Hopf oscillator as in equations (3.4) we obtain the two Lyapunov exponents $\lambda_1 = 0$ and $\lambda_2 = -c\eta^2$.

Now, using the parameters of the studies of Rinaldi et al. we can compute numerical values for the Lyapunov exponents. For the seasonal forcing via Hopf oscillator on a Rosenzweig-MacArthur system we asume a seasonality strength of $\eta = 0.5$ and a contraction value of $c = 20$. We obtain the values for two of the Lyapunov exponents $\lambda_1 = -0.0037$ and $\lambda_2 = -10.086$ in already very good agreement with the theoretical values of $\lambda_1 = 0$ and $\lambda_2 = -c\eta^2 = 10$. And the other two non-trivial Lyapunov exponents are

unchanged from a two-dimensional model.

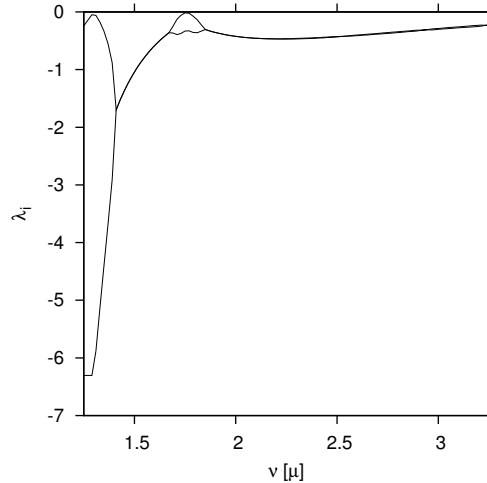## 4.4.1 Attractor Tracking

Figure 4.3: Lyapunov spectrum for small seasonal forcing $\eta = 0.1$ with Lyapunov exponents occasionally close to zero, indicating a torus as attractor.

For small seasonal forcing $\eta = 0.1$ and parameters as used by Rinaldi et al. we get a Lyapunov spectrum as depicted in figure 4.3. Here we see what can be interpreted as a Hopf bifurcation at around $\nu = 1.8\mu$ as one Lyapunov exponent gets close to zero while the other is negative.

Yet zooming into the parameter region shows irregularities in an otherwise smooth curve as can be seen in figure 4.4. These irregularities are due to numerical errors that when starting from the same initial values lead to jumps into a neighboring trajectory that is converging into a different attractor.

To avoid these jumps between coexisting attractors we change the initial values on each calculation of the Lyapunov exponents to the final values of the calculation on the step before. Starting on the first step with the initial values $X_0(t_0)$ and $Y_0(t_0)$, at the end of the calculation of the first Lyapunov exponents we end with values $X_0(T_{max})$ and $Y_0(t_{max})$ with $t_{max} := N_t \Delta t$. Now, in the next step we start the calculation at the initial values $X_1(t_0) = X_0(t_{max})$ $Y_1(t_0) = Y_0(t_{max})$. And on the i-th step we start with the initial
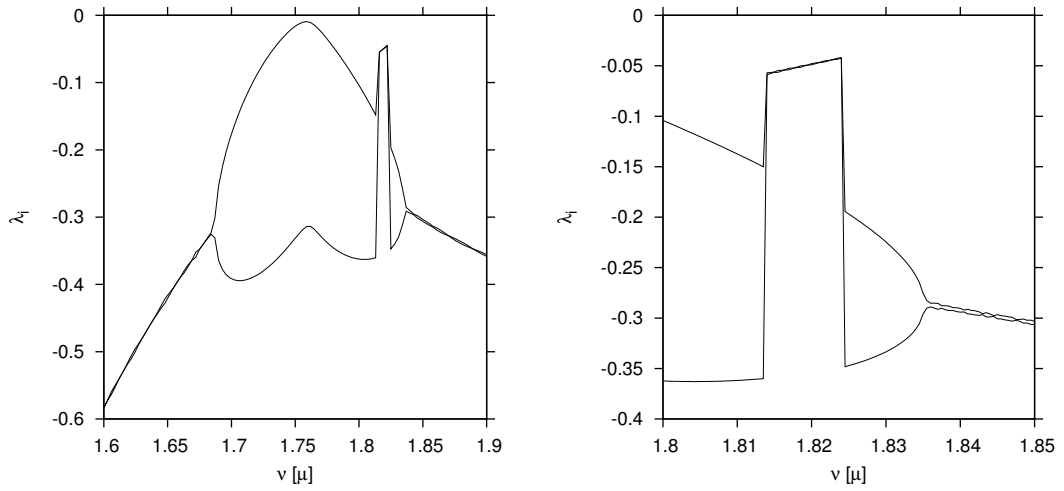
Figure 4.4: Zooming into the parameter space reveals co-existing attractors around the region of the torus bifurcation. For inital values $X(t_0) = 0.167$ and $Y(t_0) = 0.0015$.

values that were the final values of the step before, $X_i(t_0) = X_{i-1}(t_m ax)$ and $Y_i(t_0) = Y_{i-1}(t_m ax)$.
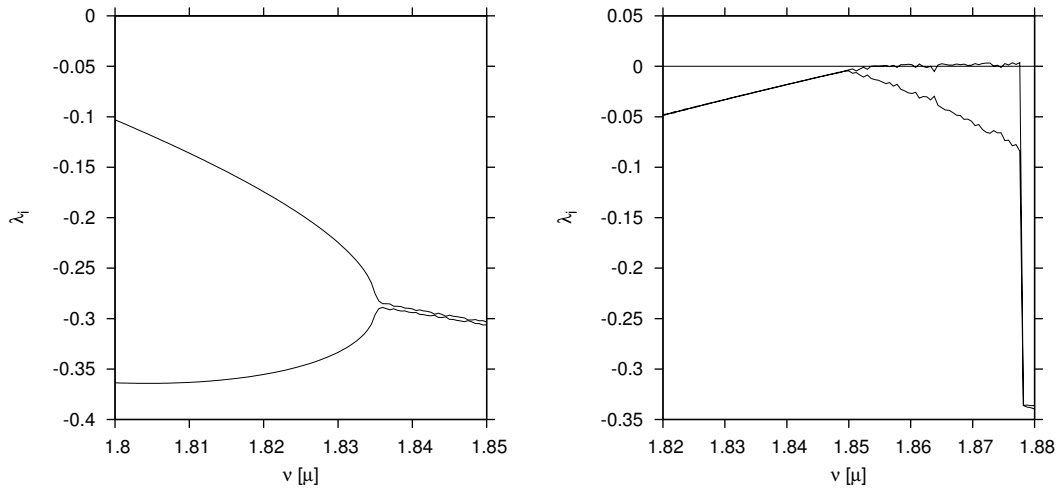

Figure 4.5: Tracking the different attractors from the initial values.

By changing the initial values for the computation of each Lyapunov expo-

nent for a different parameter ν_0 we make sure that the trajectories followed to do the computation stay in the same attractor. Hence we track one of two coexisting attractors by specifying the initial values on the first computation $X_0(t_0)$ and $Y_0(t_0)$.

The Lyapunov spectrum given with fixed initial values $X_0(t_0) = 0.380010$ and $Y_0(t_0) = 0.162432$ used to track the torus is given in figure 4.5 on the right graphic. Now, here we can clearly see the torus given by one Lyapunov exponent being zero and the other one negative.

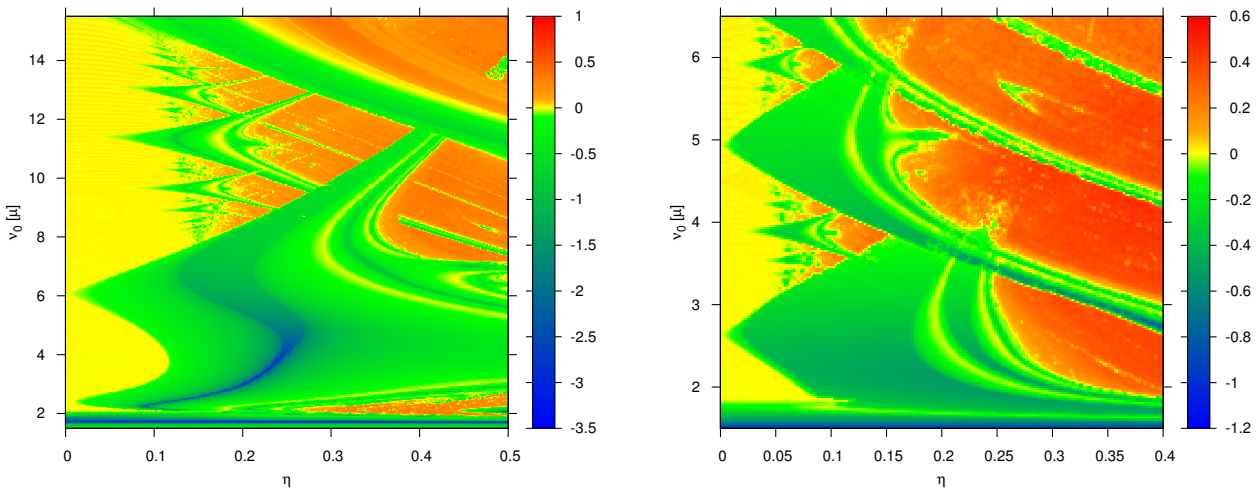## 4.5 Lyapunov Spectra for Two-Dimensional Parameter Space

Figure 4.6: Lyapunov characteristic exponents for two varying parameters, the mean predator birth eat μ_0 and the seasonality η. On the left with parameters that allow a time scale separation. On the right with parameters as useb by Rinaldi et. al. [12]

Since the dynamics of the system are given by the value of its dominant Lyapunov exponent, it is in our interest now to investigate the values of said
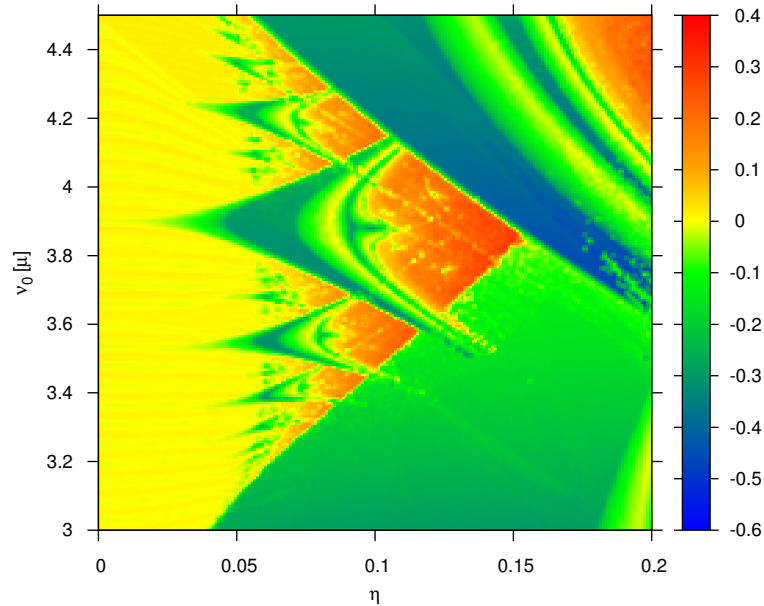
Figure 4.7: Zooming into the parameter region that displays the Arnol'd tongues. Parameters set as used by Rinaldi et. al. [12].

dominant exponent in two-dimensional parameter space. We vary now the seasonality strength η and the mean predator birth rate ν_o.

In figure 4.6 we display the Lyapunov characteristic exponents in the two dimensional parameter space coded in a color scale from blue to red. In yellow the non-trivial dominant Lyapunov exponents are zero and it indicates torus attractors, in blue and green the negative non-trivial dominant Lyapunov exponents are negative and indicate limit cycles (the yellow or light green lines inside green areas indicate limit cycle bifurcations) and in orange and red the positive dominant Lyapunov exponents indicate chaotic attractors.

The green wedges of negative dominant non-trivial exponents in the large yellow areas of zero non-trivial exponents indicate the Arnol'd tongues of

limit cycles on the tori. They can be seen more detailed when zooming into the right parameter region as in figure 4.7.

Only in these Arnol'd tongues we find characteristic exponents indicating bifurcations into chaotic dynamics, i.e. positive Lyapunov exponents in orange and red, hence the phase locking on the tori breaks up into more than two dimensional dynamic attractors, since three dimensions are needed for deterministic chaos to allow non-returning attractors different from limit cycles.

We have shown the existence of deterministic chaotic dynamics through torus break up also for parameter values which allow a time scale separation from a more complex stoichiometric system to the two-dimensional Rosenzweig-MacArthur model. This allows in future studies the analysis of stochastic systems derived from such a stoichiometric system. So we can analyze the stochastic behaviour around the torus bifurcation and torus break up into deterministic chaos. This is of major interest especially in analyzing real world systems and empirical data to perform parameter estimation.

Conclusion

We have presented the Rosenzweig-MacArthur model as a predator-prey model with additional classes of handling and searching predators. Through a time scale separation argument we showed similarities between the dynamical behavior of the extended model and the classical two dimensional Rosenzweig-MacArthur model.

This extended model proved to be useful to derive a stochastic process from the stoichiometric system. Hence, we used this extended model to perform stochastic simulations in the form of a master equation and a Fokker-Planck equation.

Following our main goal to perform an analysis of uprising Torus bifurcations we added seasonal variation to our model. We implemented this via direct forcing and via Hopf oscillator. With the additional seasonal variation we could examine the Hopf bifurcation turn into a Torus bifurcation.

In order to examine the dynamical behaviour beyond the observed torus we analyze the Lyapunov spectrum of the model. The computation of the Lyapunov spectrum of the seasonally forced revealed coexisting attractors for small seasonal variation. Throughout attractor tracking we could compute the Lyapunov exponent of coexisting attractors, showing positive Lyapunov exponents beyond the torus, hence chaotic dynamical behaviour due to torus destruction.

We focussed our further analysis in the characteristic Lyapunov exponent since it is the carrier of relevant information about bifurcations. Finally, we can perform an analysis of the characteristic Lyapunov exponents on a two dimensional parameter space. This analysis shows that the chaotic regions appear only behind wedges of stable limit cycles on the torus attractors. These wedges turned out to be the Arnol'd tongues.

In further studies the discovered coexisting multiple attractors can be analyzed in greater detail. Also more detailed profound investigations on the stochastic processes can be carried out, specifically for the parameter regions with stoichiometric systems that are now possible. Also, more complex pop-

ulation biological systems, e.g. epidemiological multi-strain models which already present torus bifurcations in autonomous systems and transitions into chaotic behaviour can be analyzed using the Lyapunov spectra as shown here additionally to classical numerical bifurcation analysis via continuation.

However, these results are encouraging for the understanding of such larger population dynamical systems. Furthermore the stochastic processes described here as master equation and Fokker-Planck equation lead to new tools for empirical data analysis.

Bibliography

[1] F. BRAUER, C. CASTILLO-CHAVEZ, *Mathematical Models in Population Biology and Epidemiology*, Springer, New York, 2001.

[2] C.W. GARDINER, *Handbook of stochastic methods*, Springer, New York, 1985.

[3] D.T. GILLESPIE, (1976) *A general method for numerically simulating the stochastic time evolution of coupled chemical reactions*, Journal of Computational Physics **22** (1976) 403–434.

[4] D.T. GILLESPIE, *Monte Carlo simulation of random walks with residence time dependent transition probability rates*, Journal of Computational Physics **28** (1978) 395–407.

[5] C. HOLLING *The functional response of predators to prey density and its role in mimicry and population regulation,* Mem. Entomol. Soc. Canada 45 (1965).

[6] P. FUENTES, L. MATEUS, B. KOOI, M. AGUIAR, N. STOLLENWERK, *Hopf and torus bifurcations in stochastic systems in mathematical population biology*, Proceedings of the 15th International Conference on Mathematical Methods in Science and Engeneering - CMMSE 2015, Cádiz, Spain, pp. 543-555 ISBN: 978-84-617-2230-3

[7] P. FUENTES, N. STOLLENWERK, B. KOOI, L. MATEUS, P. GHAFFARI, M. AGUIAR, *Lyapunov Spectra for Torus bifurcations and Ways to Deterministic Chaos in Population Biology*, Proceedings of the 16th International Conference on Mathematical Methods in Science and Engeneering - CMMSE 2016, Cádiz, Spain, pp. 491-498 ISBN: 978-84-617-2230-3

[8] A. J. LOTKA, *Elements of Physical Biology*, Williams & Wilkins Company, Baltimore, 1925.

[9] A. NORDSIECK, E. LAM, G. UHLEMBECK, *On the Theory of Cosmic-Ray Showers in the Furry Model and the Fluctuation Problem*, Physica VII, no4 (1940) pp. 344–360.

[10] U. PARLITZ, *Identification of True and Spurious Lyapunov Exponents from Time Series*, International Journal of Bifurcation and Chaos (1992) pp. 155–165.

[11] N.G. VAN KAMPEN, *Stochastic Processes in Physics and Chemistry*, North-Holland, Amsterdam, 1992.

[12] S. RINALDI, S. MURATORI, Y. KUZNETSOV, *Multiple attracttors, catastrophes and chaos in seasonally perturbed predator-prey communities*, Bulletin of Mathematical Biology,**55** (1993) 15–35.

[13] F. ROCHA, M. AGUIAR, M. SOUZAAND, N. STOLLENWERK, *Time-scale separation and center manifold analysis describing vector-borne disease dynamics*, Int. Journal. Computer Math. **90** (2013) 2105–2125.

[14] N. STOLLENWERK AND V. JANSEN, *Population Biology and Criticality*, Imperial College Press, World Scientific, London, 2011.

[15] N. STOLLENWERK, P. FUENTES, L. MATEUS, B. KOOI & M. AGUIAR (2015) Stochastic Hopf and torus bifurcations in population biology, *ICNAAM, Numerical Analysis and Applied Mathematics, International Conference 2015, Rhodes, Greece*, edited by T.E. Simos, G. Psihoyios, and Ch. Tsitouras, American Institute of Physics.

[16] N. STOLLENWERK, P. FUENTES, B. KOOI, L. MATEUS, P. GHAFFARI, M. AGUIAR *Hopf and torus bifurcations, torus destruction and chaos in population biology* Submitted for publication (2016)